IIASA

International Institute for Applied Systems Analysis • A-2361 Laxenburg • Austria
Tel: +43 2236 807 • Fax: +43 2236 71313 • E-mail: info@iiasa.ac.at • Web: www.iiasa.ac.at

INTERIM REPORT IR-97-083 / November

Pandemics of Focal Plant Disease: A Model

F. van den Bosch (frank@rcl.wau.nl)
J.A.J. Metz (metz@rulsfb.LeidenUniv.nl)
J.C. Zadoks (JCZadoks@User.DiVa.nl)

Approved by
Ulf Dieckmann (dieckman@iiasa.ac.at)
Project Coordinator, *Adaptive Dynamics Network*

Contents

Abstract

An analytical model of a pandemic, initiated by a single focus and spreading over a continent, is developed, using foci as the smallest units of disease and fields as the smallest units of host. A few generalizing assumptions lead to a parameter sparse model which may answer general questions on pandemics in a qualitative manner. For pandemic spread of disease during one season a 'within-season velocity of pandemic spread', C, is expressed in a set of integral equations. Reduction of inoculum during the off-season is expressed by a 'survival ratio' of inoculum, ε. The effect of the off-season is a 'push-back' of the pandemic front over a distance Δh. It will be shown how Δh is related to C and ε. The mean pandemic spread over successive years is calculated as the 'polyetic velocity of pandemic spread', V, which depends on C and the push-back distance. The concept of 'pandemic effectiveness' is parameterized. Relations between the two velocities of pandemic spread and several model parameters are studied. Velocities of pandemic spread depend in a limited way on field density represented by the 'cropping ratio' ζ. A general conclusion is that eradication and containment of a beginning pandemic becomes more difficult when the pandemic effectiveness of the disease is high, the tail of the spore dispersal probability distribution is long, the sanitation during the off-season is poor, and the growing or epidemic season is long.

Keywords: analytical model, effectiveness, disease spread, focus, plant disease, overseasoning, pandemic, seasonality.

Pandemics of Focal Plant Disease: A Model

F. van den Bosch
J.A.J. Metz
J.C. Zadoks

1 Introduction

Several plant diseases are present in certain areas of the world but absent from others. Some of these diseases may cause great economic loss when they invade new areas. As a precaution, expensive quarantine measures are taken. Once a quarantine disease has invaded an area, containment and eradication may be attempted. When these measures fail the disease will spread from the point of introduction till it reaches regions where, due to adverse climatic conditions or the absence of the host crop, further expansion comes to a stop.

An epidemic expanding over a continent is called a pandemic (Gäumann, 1946). A well documented example of a pandemic is that of tobacco blue mold (*Peronospora tabacina*). The fungus existed in Australia in the 19th century (Cooke, 1891) and was reported in the United States in 1921. Between 1931 and 1950 a pandemic took place in North America. The velocity of pandemic spread was approximately 50 km per year (Zadoks and Kampmeijer, 1977). The disease did not appear in Europe until 1959 when it was first found in England. It spread within five years over continental Europe and the mediterranean countries (Populer, 1964). Losses were worst in the mediterranean countries with records of up to 75% in Algeria and 65% in Italy. The velocity of pandemic spread was approximately 130 km per year (Zadoks and Kampmeijer, 1977).

In his work on emigrant pests McGregor (1978) stated that estimation of the relative danger posed by a quarantine pest and the design of emergency measures for containment and eradication would profit from models of pandemics with at least some predictive value. The point was raised again by Heesterbeek and Zadoks (1987), who performed a preliminary analysis of the present knowledge on pandemic spread. No model of pandemic spread has been formulated and analyzed to date.

The modeling of population expansion in space has a tradition in ecology and population genetics, beginning with Fisher (1937) and Skellam (1951). Kendall (1965) was the first to apply models to the study of spatial spread of diseases. A general model for the spatial expansion of age structured populations was developed by Diekmann (1978, 1979) and Thieme (1977). Van den Bosch *et al.* (1990a) and Metz and van den Bosch (1995) operationalized this model and analyzed invasions by several vertebrate species. Zadoks and Kampmeijer (1977) studied epidemic spread

by means of the spatially structured simulation model EPIMUL. Minogue and Frey (1983a,b) were the first to apply simple analytically tractable models in their study of the expansion of a plant disease in a one-dimensional planting. Van den Bosch *et al.* (1990a) studied the two-dimensional expansion of plant disease foci (van den Bosch *et al.*, 1988a,b,c, 1990b).

In this paper we will show that the step from analyzing small-scale spatial disease expansion to large-scale pandemics of focus forming plant diseases is feasible. Focus formation is a short-time and small-scale phenomenon where time and space are assumed to be continuous. For pandemic expansion this assumption no longer holds. Epidemic progress within the field, consisting of both focus expansion and initiation of new foci, is essentially different from the epidemic development in an assemblage of distant fields. Moreover, pandemics usually need several successive cropping seasons. Although it is a reasonable first approximation to consider a continuous time model for the expansion within one cropping season, we cannot ignore the discontinuity of time for pandemic expansion due to periods, usually winters, where disease development and spread is not possible. In this paper we show how these aspects can be incorporated into a model. We will show how the velocity of pandemic spread within one cropping season and the mean velocity during successive cropping seasons relate.

2 Model and Methods

In this section a model is derived for the spatial expansion of a focal plant disease. We limit the discussion to polycyclic fungal disease propagated by air-borne spores. A summary of variables, parameters and interpretations is given in Table 1.

Continent. A pandemic spreads over a continent. A continent is considered to be an infinitely large two-dimensional space. Position in space will be given in the usual cartesian coordinate system (x_1, x_2). We will often use a shorthand notation $\vec{x} = (x_1, x_2)$.

Crop. A crop is the agronomic entity grown continent-wide and susceptible to the disease under consideration. A crop occupies fields. Fields are assumed to be randomly distributed over the continent.

Field. A field is the geographical entity carrying a crop, with a position (x_1, x_2). All fields are assumed to be equal in size and in accessibility to incoming spores, disease susceptibility, escapeability of outgoing spores, climatic conditions and cropping season.

Target area. The target area is the part of the continent covered by fields planted with the crop susceptible to the disease considered, the non-target area is the part not covered by such a crop. The ratio of target area to total area will be called 'the cropping ratio', ζ.

Season. The year consists of a cropping season and an off-season. The cropping season, shortly season, is the part of the year when fields are covered by the crop so that the epidemic can proceed. The off-season is the part of the year when there is no crop available.

Table 1. Definitions of the variables and parameters used in the model.

Variables		
$\rho(t, \vec{x})$	Number of spores produced per unit of time by a field at position $\vec{x} = (x_1, x_2)$ at time t (field rate of spore production).	$[\mathrm{N_s} \cdot \mathrm{T}^{-1} \cdot \mathrm{L}^{-2}]$[a]
$b(t, \vec{x})$	Number of foci initiated per unit of time in a field at position $\vec{x}$ at time t (rate of focus initiation).	$[\mathrm{N_f} \cdot \mathrm{T}^{-1} \cdot \mathrm{L}^{-2}]$
$\nu(t, \vec{x})$	Number of between-field spores deposited per unit of time at position $\vec{x}$ and at time t (rate of spore deposition).	$[\mathrm{N_s} \cdot \mathrm{T}^{-1} \cdot \mathrm{L}^{-2}]$
$N(t, \vec{x})$	Number of foci in a field at position $\vec{x}$ at time t.	$[\mathrm{N_f} \cdot \mathrm{L}^{-2}]$
Functions		
$g(a)$	Number of spores produced per unit of time by a focus of age a (focus rate of spore production).	$[\mathrm{N_s} \cdot \mathrm{T}^{-1}]$
$D(\vec{x}, \vec{\varphi})$	The probability density of a between-field spore originating from a field at position $\vec{\varphi}$ to be deposited in a field at position $\vec{x}$ (pandemic dispersal distribution).	$[\mathrm{N_s} \cdot \mathrm{L}^{-2}]$
$F(a)$	Number of foci initiated per unit of time due to (within-field and between-field) spores produced by a field infected time a ago.	$[\mathrm{N_f} \cdot \mathrm{T}^{-1}]$
Parameters		
a	Time since the initiation of a focus, age of a focus.	[T]
α	Parameter in the spore production function $g(a)$	$[\mathrm{N_s} \cdot \mathrm{T}^{-2}]$ in (16); $[\mathrm{N_s} \cdot \mathrm{T}^{-1}]$ in (17)
$\alpha\Psi$	Measure of pandemic effectiveness.	$[\mathrm{N_f} \cdot \mathrm{T}^{-2}]$ in (16); $[\mathrm{N_f} \cdot \mathrm{T}^{-1}]$ in (17)
C	Within-season velocity of pandemic spread.	$[\mathrm{L} \cdot \mathrm{T}^{-1}]$
ε	Probability of a focus to survive the off-season (survival ratio).	$[\mathrm{N_f} \cdot \mathrm{N_f}^{-1}]$
ζ	Fraction of the continent covered by host fields (cropping ratio).	[1]
κ	Probability that a spore leaving the canopy is redeposited in the field of its origin (probability of within-field spore dispersal).	[1]
λ	Steepness parameter of the pandemic disease profile.	$[\mathrm{L}^{-1}]$
σ	Standard deviation of pandemic dispersal density, $D(\vec{x}, \vec{\varphi})$.	[L]
t	Time.	[T]
T	Duration of the crop season.	[T]
V	Polyetic velocity of pandemic spread.	$[\mathrm{L} \cdot \mathrm{T}^{-1}]$
$\vec{x} = (x_1, x_2)$	Position on the two-dimensional continent.	[L]
Ψ	Probability that a spore landing in a field initiates a new focus (the success ratio).	$[\mathrm{N_f} \cdot \mathrm{N_s}]$

[a] 1 = no dimension, L = length, $\mathrm{N_s}$ = number of spores, $\mathrm{N_f}$ = number of foci, T = time.

2.1 Spatial spread within one cropping season

Individual. In modeling the dynamics of an infectious disease one usually takes the (biological) individual as the conceptual unit for modeling. For plant disease such an individual can be a fungal spore, a lesion, an infected leaf or an infected plant. For modeling a pandemic such a definition of individual is not suited. The methods to calculate the velocity of spatial population expansion developed by Diekmann (1978) and van den Bosch *et al.* (1990a) assume that density dependence in the tail end of the epidemic is negligible. However, in focal plant disease a non-negligible depletion of susceptibles inside a focus will certainly occur, even in the tail end of the epidemic. We circumvent this problem by taking the focus as our generalized individual and conceptual unit of modeling.

Fate of a spore. We discuss disease transmitted by air-borne spores. Spores dispersed inside the canopy contribute to the development of the focus from which they originate but they do not contribute to the initiation of new foci, i.e., new individuals. We only consider spores which temporarily leave the canopy so that they can initiate new foci when landed elsewhere.

Consider a focus initiated time a ago. We will loosely speak of a as 'the age of the focus'. The number of spores leaving the canopy depends on focal age, a. By $g(a)$ we denote the number of spores (per unit of time), produced by a focus of age a, which leave the canopy. A spore leaving the canopy can be re-deposited in the field where it originated with a probability κ. These spores will loosely be called 'within-field spores'. With probability $1-\kappa$ a spore becomes subject to between-field dispersal so that it can initiate a new focus in another, maybe distant, field. Such spores are called 'between-field spores'. The different modes of dispersal are depicted in Figure 1 (top). Thus we distinguish within-field dynamics and between-field pandemic spread of the disease.

To describe the between-field dispersal of spores we introduce the spore dispersal density $D(\vec{x},\vec{\varphi})$. This probability density is the probability that a spore originating from a source field at position $\vec{\varphi}$ is deposited in a target field at position $\vec{x}$. We assume that dispersal has no preferred direction and that dispersal is the same in every position on the continent. This implies that the dispersal probability only depends on the distance between the positions of source and target fields, $\vec{\varphi}$ and $\vec{x}$. We write

$$D(\vec{x},\vec{\varphi}) = D(|\vec{x}-\vec{\varphi}|) \quad ,$$

where $|\vec{x}-\vec{\varphi}| = \sqrt{(x_1-\varphi_1)^2+(x_2-\varphi_2)^2}$, is the distance between $\vec{x}$ and $\vec{\varphi}$.

Model development. Figure 1 (bottom) summarizes the dynamics of the pandemic. A field at position $\vec{x}$ at time t can contain several foci of various ages. Each of these foci produces spores with rate $g(a)$. The total number of spores produced by the field per unit of time is denoted by $\rho(t,x_1,x_2) = \rho(t,\vec{x})$. A fraction κ of these spores is redeposited in the field (within-field spores). Not every spore of the fraction $1-\kappa$, representing the between-field spores, will be deposited in a target field since only a

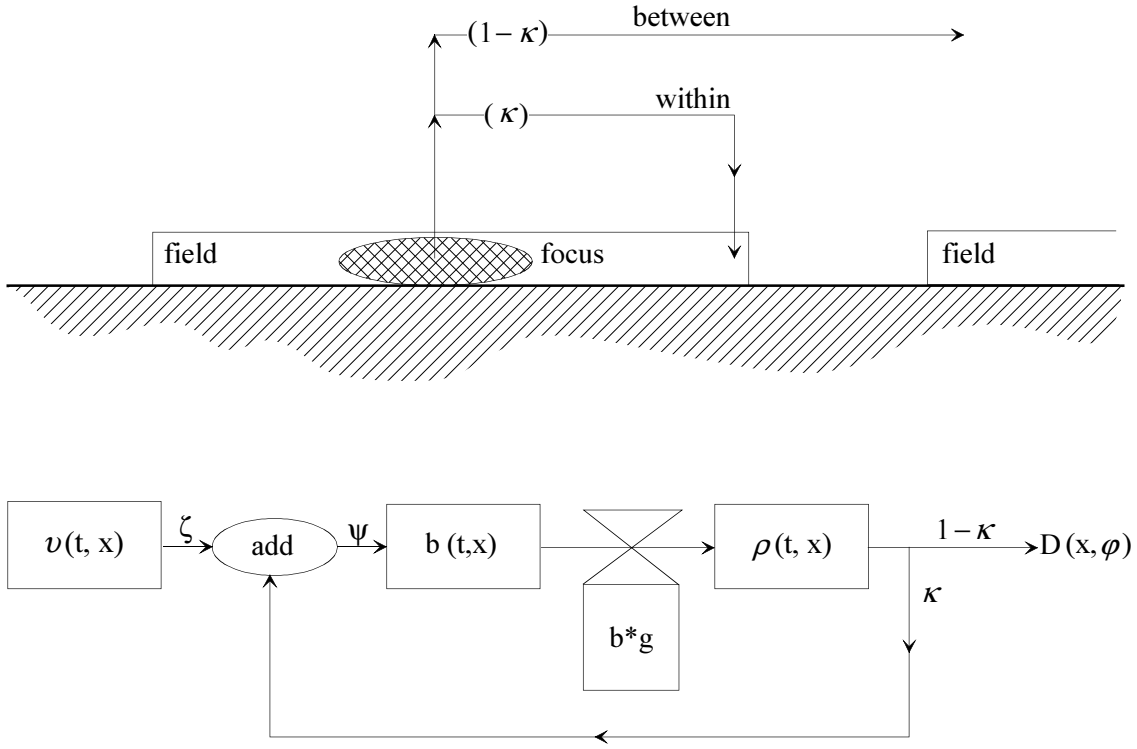

Figure 1. Graphical representation of the model structure. Symbols are explained in Table 1. Top = The fate of a spore. Bottom = The model.

fraction ζ of the continent is covered with host fields. The parameter ζ will be called the 'cropping ratio' of the continent. The total number of spores dispersed between fields, originating from all possible fields on the continent, deposited per unit of time in a field at position $\vec{x}$ is denoted by $\nu(t, x_1, x_2) = \nu(t, \vec{x})$. Both between-field spores and within-field spores can initiate new foci in the crop at position $\vec{x}$. The probability that a spore landing in a field initiates a new focus is denoted by Ψ. The number of new foci initiated per unit of time per unit of area in a field at position $\vec{x}$ at time t is denoted by $b(t, x_1, x_2) = b(t, \vec{x})$. Note that ν, b and ρ are numbers per unit of time, or rates per unit area.

To calculate the total rate of spore production of a field, $\rho(t, \vec{x})$, we first consider foci of age a in this field. The number of foci of age a equals the number of foci initiated at time $t-a$, $b(t-a, \vec{x})$. These foci together produce $g(a)b(t-a, \vec{x})$ spores per unit of time. Foci of all possible ages contribute to the total rate of spore production of a field, $\rho(t, \vec{x})$. To calculate $\rho(t, \vec{x})$ we therefore must add all contributions of all focus ages to arrive at

$$\rho(t, \vec{x}) = \int_0^\infty b(t - a, \vec{x}) g(a) da \quad . \tag{1}$$

The total number of spores deposited per unit of time in a field at position $\vec{x}$ at time t is the sum of within-field spores, S_1, and between-field spores, S_2. Given the probability of a spore deposited in a field to initiate a new focus, Ψ, the number of foci initiated per unit of time, $b(t, \vec{x})$, equals

$$b(t,\vec{x}) = \Psi\,(S_1 + S_2) \tag{2}$$

The parameter Ψ will be called 'the success ratio'. The deposition rate of within-field spores is $S_1 = \kappa\rho(t,\vec{x})$ and the deposition rate of between-field dispersed spores $S_2 = \nu(t,\vec{x})$.

Model completion. To complete the model we derive a relation between the deposition rate of between-field spores in a field at $\vec{x}$ and the spore production rate of fields all over the continent. Consider a field at position $\vec{\varphi}$. This field produces $(1-\kappa)\rho(t,\vec{\varphi})$ between-field spores per time unit. The number of spores originating from $\vec{\varphi}$ and deposited at $\vec{x}$ equals $(1-\kappa)\rho(t,\vec{\varphi})D(\vec{x},\vec{\varphi})$. Multiplying this value by the cropping ratio, ζ, yields the number of between-field spores originating from a source field at $\vec{\varphi}$ and deposited in target fields at position $\vec{x}$. To calculate the total number of spores deposited per unit of time in target fields at $\vec{x}, \nu(t,\vec{x})$, we have to add all contributions of fields at all possible places $\vec{\varphi}$. The expression for $\nu(t,\vec{x})$ thus is:

$$\nu(t,\vec{x}) = \zeta(1-\kappa)\int_{-\infty}^{\infty}\int_{-\infty}^{\infty}\rho(t,\vec{\varphi})D(\vec{x},\vec{\varphi})d\varphi_1 d\varphi_2 \quad . \tag{3}$$

Putting all pieces together and substituting equation (1) where appropriate the model finally reads:

$$\begin{aligned} b(t,\vec{x}) &= \Psi\nu(t,\vec{x}) + \Psi\kappa\int_0^{\infty} b(t-a,\vec{x})g(a)da \\ \nu(t,\vec{x}) &= \zeta(1-\kappa)\int_0^{\infty}\int_{-\infty}^{\infty}\int_{-\infty}^{\infty} b(t-a,\vec{\varphi})g(a)D(\vec{x},\vec{\varphi})d\varphi_1 d\varphi_2 da \quad . \end{aligned} \tag{4}$$

If one is not interested in the rate at which new foci are initiated in a field at position $\vec{x}$ but in the number of foci in this field, $N(t,\vec{x})$, this can be calculated from

$$N(t,\vec{x}) = \int_0^{\infty} b(t-a,\vec{x})da \quad .$$

Reformulation of the model. Appendix I shows that, using Laplace transformation, the model can be rewritten as

$$b(t,\vec{x}) = \int_0^{\infty}\int_{-\infty}^{\infty}\int_{-\infty}^{\infty} b(t-a,\vec{x})F(a)D(\vec{x},\vec{\varphi})d\varphi_1 d\varphi_2 da \quad , \tag{5}$$

where

$$F(a) = \phi\frac{1-\kappa}{\kappa}\sum_{i=1}^{\infty}(\kappa\Psi)^i g^{*i}(a) \quad . \tag{6}$$

In equation (6) the term $g^{*i}(a)$ is the so-called convolution of i times the function $g(a)$, defined as

$$g^{*i}g(a) = \int_0^a g(\tau)g^{*(i-1)}(a-\tau)d\tau \quad , \tag{7}$$

for $i = 2, 3, \ldots$ and $g(a)^{*1} = g(a)$.

Velocity of pandemic spread. The model in its reformulated form (5) is a general model often used to study the spread of animal, plant and pathogen populations. This model and its non-linear variants are extensively studied by various authors (Diekmann, 1978, 1979; Thieme, 1977; Van den Bosch *et al.*, 1988abc, 1990ab; Mollison 1991; Metz and Van den Bosch, 1995). We refer the reader to these publications for details on the mathematical analysis of equation (5). Here we state the main results to be used in this paper.

Since the between-field dispersal density is rotationally symmetric, the pandemic has circular symmetry too. Therefore, the following can be limited to a transect along the x_1-axis. When a new disease is locally introduced in a continent the epidemic will spread over the continent as a travelling wave (Zadoks and Van den Bosch, 1994). Such a travelling wave can be visualized as a disease profile with a fixed shape in space. This disease profile moves through space at a constant velocity. The disease profile of the travelling wave solution of equation (5) has an exponential shape given by

$$b(t, x_1, 0) = Me^{\lambda(Ct - x_1)} \quad , \tag{8}$$

where C is the velocity of the travelling wave, λ is the steepness parameter of the disease profile and M is a parameter (Figure 2A).

The results reported in the literature on equation (5) imply that the velocity, C, and steepness, λ, of the (only relevant) travelling wave solution can be calculated from

$$\begin{cases} L(C,\lambda) &= 1 \\ \frac{\partial L(C,\lambda)}{\partial \lambda} &= 0 \end{cases} \quad , \tag{9}$$

where

$$L(C,\lambda) = \int_0^\infty e^{-\lambda C a}F(a)da \int_{-\infty}^\infty e^{\lambda x_1}\tilde{D}(x_1)dx \quad , \tag{10a}$$

is the characteristic equation and

$$\tilde{D}(x_1) = \int_{-\infty}^\infty D(x_1, x_2)dx_2 \tag{10b}$$

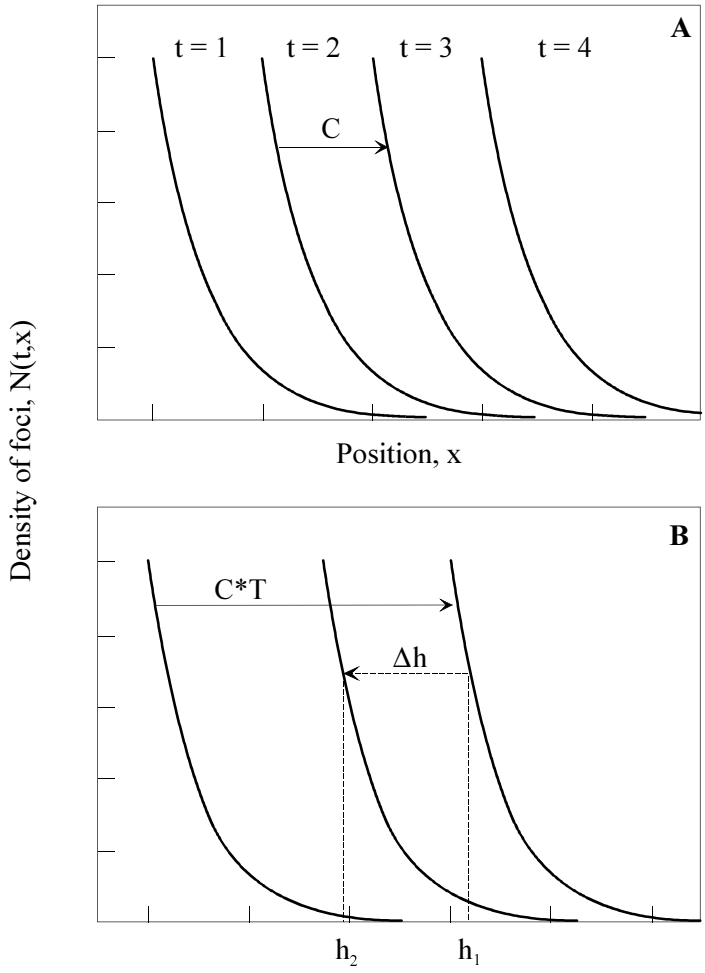

Figure 2. Rate of focus initiation, $b(t, x)$, or density of foci, $N(t, x)$, as function of position. A = The pandemic disease profile for various moments, t, during one cropping season. C is the within-season velocity of pandemic spread. B = The development of the pandemic profile during one year. Left most curve: pandemic disease profile at the onset of the cropping season. Right most curve: pandemic disease profile at the end of the cropping season/at the start of the off-season. Middle curve: pandemic disease profile at the end of the off-season. C^*T is the total distance travelled by the pandemic wave during one cropping season. ε is the probability of a focus to survive the off-season. The left-pointing dotted arrow indicates the push-back distance, Δh.

is the marginal distribution of the spore dispersal density, $D(\vec{x})$. Note that calculating the within-season velocity of pandemic spread, C, is only possible if the integrals in equation (10a) exist. This condition does not cause problems with the functions $F(a)$ and $g(a)$ but it imposes a biologically relevant restriction on the second integral of equation (10a), which only exists when the tail of $D(\vec{x})$ falls off exponentially or steeper with increasing $\vec{x}$.

2.2 Spread during successive cropping seasons

Model (4) describes the epidemic expansion within one cropping season. The duration of a cropping season will be denoted by T. During one cropping season the epidemic wave travels a distance CT. Again considering a transect along the x_1-axis, the pandemic disease profile at the end of the cropping season, at time $t = T$ is

$$N(T, x_1, 0) = Ne^{\lambda(CT - x_1)} \quad , \tag{11}$$

where N is the number of foci in a field at position $\vec{x}$. At the end of the cropping season, $t = T$, the crop is harvested and most inoculum is removed from the field. The remaining inoculum now has to survive the off-season on plant parts not removed during harvest, on cull piles, as for *Phytophtora infestans*, or on secondary hosts. Only a fraction of the inoculum will survive the off-season. At the start of the next cropping season the surviving inoculum can induce one or more new foci. We will denote by ε the number of foci at the beginning of a cropping season relative to the number of foci at the end of the preceding cropping season. We will loosely speak of ε as the 'survival ratio' of foci. The disease profile at the start of the next cropping season equals disease profile (11) multiplied by ε,

$$N(T, x_1, 0) = \varepsilon Ne^{\lambda(CT - x_1)} \quad . \tag{12}$$

Equation (12) implies that the steepness of the pandemic disease profile has not changed during the off-season. The effect of the off-season is only to push back the disease profile over a certain distance (Δh in Figure 2B). To calculate this distance consider a position h_1 where at the end of the cropping season the density of foci in a field is θ. At the start of the next cropping season this same disease level θ now has position h_2. Substituting in equations (11) and (12) we find

$$Ne^{\lambda(CT - h_1)} = \varepsilon Ne^{\lambda(CT - h_2)} \quad , \tag{13}$$

and the push-back distance Δh is

$$\Delta h = h_1 - h_2 = \frac{1}{\lambda} \ln\left(\frac{1}{\varepsilon}\right) \quad . \tag{14}$$

The mean velocity of pandemic spread over a continent during successive cropping seasons, V, here called the 'polyetic velocity of pandemic spread', is the distance

travelled during a cropping season, CT, minus the push-back distance. Therefore V is calculated from

$$V = CT - \frac{1}{\lambda} \ln \left(\frac{1}{\varepsilon} \right) \quad , \tag{15}$$

where C and λ are calculated from (9), (10).

2.3 Choosing submodels

To actually calculate the velocity of pandemic spread from model (4), using equations (9) and (10), the functions $g(a)$ and $D(\vec{x})$ have to be specified. In this section we introduce simple parameter sparse submodels for these two functions. By comparing velocities of pandemic spread for these submodels we get insight in the influence of the details of the spore production, $g(a)$, and spore dispersal, $D(\vec{x})$, functions on the velocity of pandemic spread.

Spore production function $g(a)$. After a build-up phase a focus expands radially at constant velocity (van den Bosch *et al.*, 1988a, 1990a). Since the amount of host material is limited a burn-out zone will develop inside the focus. Thus we distinguish three circular zones:

(1) An outer zone where disease severity is so low that the contribution to spore production is negligible. (2) An intermediate zone, the productive zone, where disease level and spore production are high. In a mature focus the width of this zone is constant. (3) A central zone, the burn-out zone, which is no longer producing spores. Since the inner and outer boundaries of the intermediate zone increase linearly with time, total area of the productive zone also increases linearly with time. Therefore we choose as a first approximation of the spore production by a focus of age a

$$g(a) = \alpha a \quad . \tag{16}$$

For reasons of comparison we choose as an alternative description

$$g(a) = \alpha \quad , \tag{17}$$

implying a constant rate of spore production by a focus.

Spore dispersal function $D(\vec{x})$. Consider the following simple description of between-field spore dispersal. Driven by wind a spore flies at a constant velocity, denoted by ν. The flight direction makes an angle θ with the positive x_1-axis. With a probability γ per unit of time the wind direction changes. The new direction, $-\pi < \theta < \pi$, is chosen at random. The spore is deposited with a probability μ per time unit. The equation describing this dispersal process is given in Appendix II. Here, we use two limiting cases of the model.

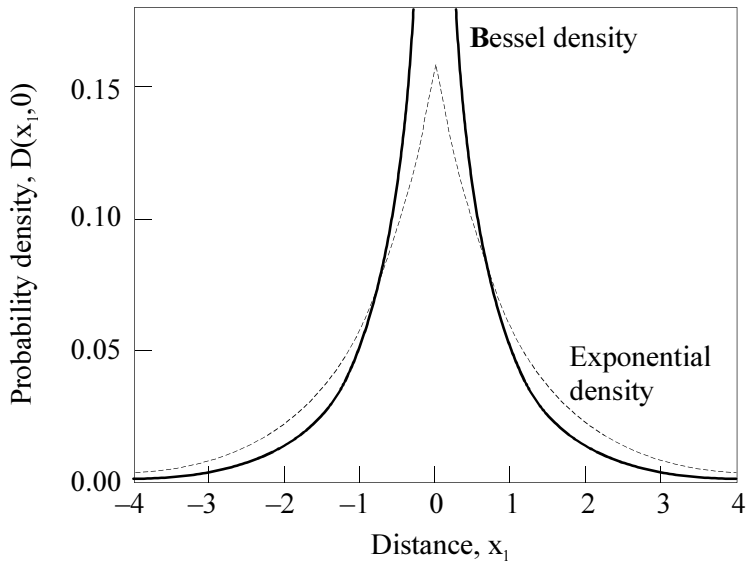

Figure 3. Transect of the between-field dispersal densities used as special cases of the general model.

When the average flight duration, $1/\mu$, is very small compared to the average duration of the air flow in a fixed direction, $1/\gamma$, the spore dispersal distribution is approximated by the exponential distribution,

$$D(\vec{x}) = \frac{1}{2\pi\sigma^2} \exp\left\{\frac{1}{\sigma}\sqrt{x_1^2 + x_2^2}\right\} \quad , \tag{18}$$

where $\sigma^2 = \nu^2/\mu^2$ is the variance of the marginal spore dispersal density (10b).

When the average time length during which a spore is air-borne, $1/\mu$, is very large compared to the average duration of travelling in a fixed direction, $1/\gamma$, the spore dispersal distribution approximately follows the Bessel-density

$$D(\vec{x}) = \frac{1}{8\pi\sigma^2} \int_0^\infty \frac{1}{\tau} \exp\left\{-\tau - \frac{x_1^2 + x_2^2}{\tau 8\sigma^2}\right\} d\tau \quad , \tag{19}$$

where $\sigma^2 = 2\nu^2/(\gamma\mu)$ is the variance of the marginal spore dispersal density (10b). This Bessel distribution has also been used by van den Bosch *et al.* (1988b) in the analysis of focus expansion. Figure 3 compares transects through the Bessel and exponential densities.

3 Results

3.1 Epidemic spread within one cropping season

The two submodels for the spore production function $g(a)$ and the two submodels for the spore dispersal density $D(x_1, x_2)$ combine to four special cases of the model. The within-season velocity of pandemic spread, C, and the steepness parameter of the

Table 2. The equations for the within-season velocity of pandemic spread, C, and the steepness parameter of the pandemic disease profile, λ, where $A = \zeta\frac{1-\kappa}{\kappa}$.

	$D(\vec{x})$ Bessel	$D(\vec{x})$ Exponential
$g(a)$ linear		*Solve Z numerically from* $Z^3 - 3Z^2 + Z\left(3 - \frac{27}{4}A^2\right) - 1 = 0$
	$C = \sqrt{\alpha\Psi}\sigma\frac{1}{\sqrt{2}}\sqrt{\kappa}\sqrt{\frac{1+A+\sqrt{A^2+A}}{1+A-\sqrt{A^2+A}}}$	*Now* $C = \sqrt{\alpha\Psi}\sigma\sqrt{\kappa Z}$ *and*
	$\lambda = \frac{1}{\sigma}\sqrt{2}\sqrt{1+A-\sqrt{A^2+A}}$	$\lambda = \frac{1}{\sigma}\sqrt{\frac{\kappa+2Z}{3Z}}$
$g(a)$ constant		*Solve Z numerically from* $Z^3 + 2AZ^2 - A = 0$
	$C = \alpha\Psi\sigma\frac{1}{\sqrt{2}}\sqrt{\kappa}\left(1 + \frac{3}{4}A + \frac{1}{4}\sqrt{9A^2+8A}\right)B$	*Now* $C = \alpha\Psi\sigma\frac{A+Z}{Z\sqrt{1-Z^2}}$ *and*
	where $B = \sqrt{\frac{3A+\sqrt{9A^2+8A}}{-A+\sqrt{9A^2+8A}}}$	
	$\lambda = \frac{\sqrt{2}}{\sigma}\sqrt{1 - \frac{4A}{3A+\sqrt{9A^2+8A}}}$	$\lambda = \frac{1}{\sigma}\sqrt{1-Z^2}$

exponential disease profile, λ, are calculated using equations (9) and (10). Table 2 summarizes the results of these straightforward but lengthy calculations. The two special cases with the Bessel distribution yield explicit solutions for C and λ. For the two cases with the exponential distribution a cubic was solved numerically by a Newton-iteration subroutine (Press *et al.*, 1992).

Table 2 shows that in all four cases the polyetic velocity of pandemic spread, V, depends linearly on the standard deviation, σ, of the marginal dispersal density. This dependence, which also follows from scaling arguments, is not a property specific to the special cases but holds for any model of the form (5) (van den Bosch *et al.*, 1990a).

In all equations for the velocity of pandemic spread Table 2 the parameter α of the spore production function and the success ratio, Ψ, appear as a product. The product $\alpha\Psi$ can be interpreted as a measure of the effectiveness (sensu Zadoks and Schein, 1979) of the pathogen. When the rate of spore production increases linearly with time the velocity of pandemic spread increases with the square root of $\alpha\Psi$. For a constant rate of spore production the velocity of pandemic spread increases linearly with $\alpha\Psi$. This difference can cause large differences in the velocity of pandemic spread. Apparently, accurate information on the precise dependence of the spore production rate on the age of the focus is crucial for quantitative predictions.

Next we consider the effects of the fractions of within-field spores, κ, and of cropping ratio, ζ, on the velocity of pandemic spread, C. Figure 4 shows the de-

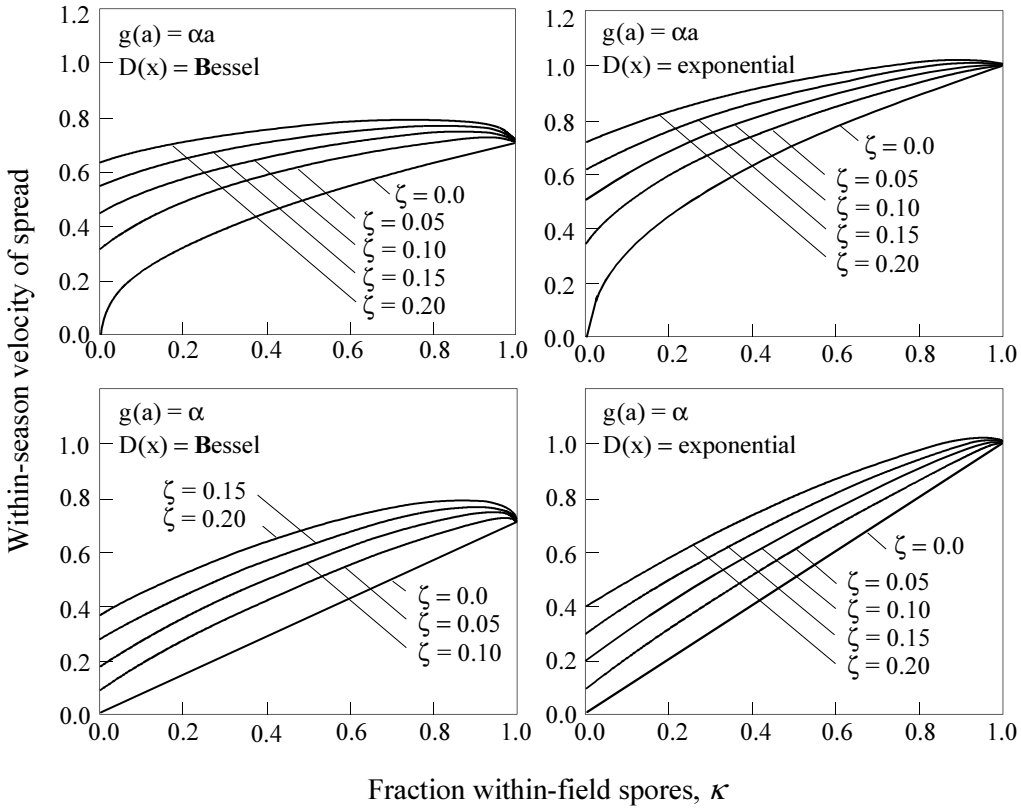

Figure 4. The within-season velocity of pandemic spread (scaled by $\sigma\sqrt{\alpha\Psi}$ for $g(a)$ is (16) and by $\sigma\alpha\Psi$ for $g(a)$ is (17)), $C/\sigma\alpha\Psi$ and $C/\sigma\sqrt{\alpha\Psi}$ respectively, as a function of the fraction of within-field spores, κ, for the four special cases studied. Parameters and functions are explained in Table 1.

pendence of the velocity on these two parameters for all four cases. There are only minor qualitative differences between the four cases. The velocity of pandemic spread increases with the cropping ratio, ζ, as expected. The effect of the fraction of within-field spores, κ, on the within-season velocity of pandemic spread is remarkable. For $k = 0$ no spores are redeposited in the field of origin. Increasing κ results in larger velocities C. This effect holds for most values of κ and ζ, except for κ values close to unity. Only for unrealistically high values of ζ ($\zeta > 0.5$) we have found continuously decreasing velocities with increasing κ values. Clearly, at low values of the cropping ratio, ζ, almost all between-field spores fail to initiate a new focus since they are not deposited in a target field. We conclude that an increased rate of growth of the epidemic in a source field contributes more to the velocity of pandemic spread than an increase in the number of between-field-dispersed spores.

Even more surprising is the observation that, when κ approaches unity, implying less and less between-field spores, the high velocity of pandemic expansion is maintained. This effect was described before by Cook (Goldwasser *et al.*, 1994) who studied the velocity of population expansion of a species consisting of mobile and immobile types, with the degree of mobility determined probabilistically at birth. He also found that an extremely small number of between-field dispersers can drive a surprisingly fast population expansion. This result implies that containment measures which try to reduce the numbers of between-field spores are bound to fail in stopping or slowing down pandemic spread.

Quantitative differences are found for the within-season velocity of pandemic spread, C, between the Bessel and the exponential dispersal densities, the velocities for the Bessel density being smaller than for the exponential density. This quantitative difference is more pronounced for larger values of κ. The difference is explained by Figure 3 where the exponential density has thicker tails than the Bessel density.

Table 2 shows that the parameters α and Ψ have no effect on the steepness, λ, of the pandemic disease profile. Clearly, the effectiveness of the disease does not affect the disease profile. The steepness of the disease profile is only influenced by factors related to the dispersal of the disease.

Figure 5 shows that the pandemic steepness parameter, λ, slightly increases with increasing κ for all four cases. The larger the fraction of within-field spores the larger the rate of focus initiation in an infected field. At the same time the infection pressure on distant fields decreases. It is obvious that under these circumstances the steepness of the pandemic disease profile increases. Increasing the fraction of target area, ζ, flattens the pandemic disease profile. This effect can be interpreted in the same sense as the effect of the fraction of within-field spores, κ. The larger ζ, the more foci are initiated at distant places relative to the number initiated in the source field, an effect that flattens the pandemic disease profile. Changing parameter values so that the velocity of pandemic spread increases can thus steepen (κ) or flatten (ζ) the disease profile.

Table 2 shows that the steepness of the disease profile usually depends on the parameter combination $\zeta(1-\kappa)/\kappa$. This combination can be interpreted as the ratio between the number of effective between-field and redeposited within-field spore or, equivalently, the ratio between the number of daughter foci in distant host fields and in the host field of the mother focus. When this ratio decreases the steepness

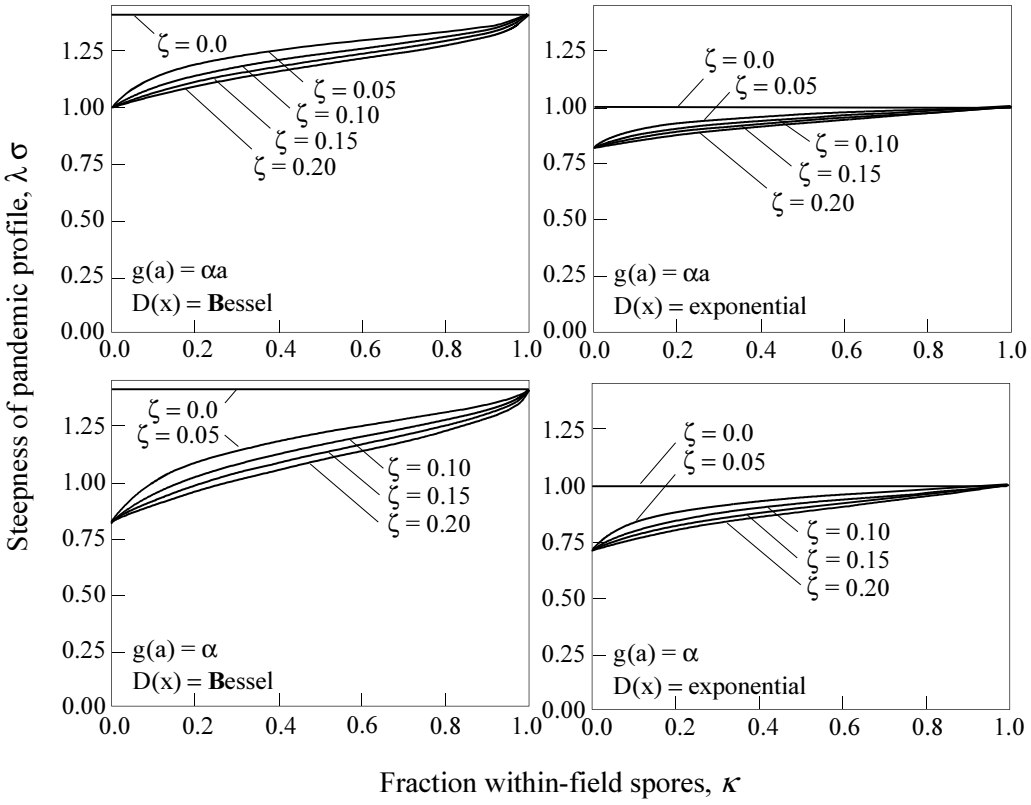

Figure 5. Steepness of the pandemic disease profile (scaled by σ), $\lambda\sigma$, as function of the fraction of within-field spores, κ, for all four special cases studied. Parameters and function explained in Table 1.

of the pandemic disease profile increases in all four cases. We conclude that the more a focus increases the growth rate of the epidemic in its own field compared to infecting distant host fields the steeper the pandemic disease profile becomes, as could be expected.

3.2 Epidemic spread during successive cropping seasons

Since the within-season velocity of pandemic spread, C, depends linearly on σ and λ depends inversely on σ (Table 2), we conclude from equation (15) that the polyetic velocity of pandemic spread, V, also increases linearly with increasing standard deviation, σ, of the marginal dispersal density, as might be expected.

Equation (14) shows that the push-back distance, Δh, during the off-season is proportional to $1/\lambda$, so that a steep pandemic disease profile is pushed back over a short distance and a flat profile is pushed back over a large distance. The equation further shows that the push-back distance is proportional to the logarithm of the fraction, ε, of the foci established after the crop-free period.

In the previous section the within-season velocity of pandemic spread, C, was analyzed. We concluded that qualitatively there was no difference between the four cases analyzed. Calculations (not shown here) indicate that this qualitative independence is also found in the polyetic velocity of pandemic spread. Therefore, we restrict our attention to the case of a Bessel dispersal density, equation (19), and a linear increase of spore production with age, equation (16). In this case:

$$V = \frac{\sigma}{\sqrt{2}} \frac{\sqrt{\alpha\Psi}\sqrt{\kappa}T\sqrt{1 + A + \sqrt{A^2 + A}} - \ln\left(\frac{1}{\varepsilon}\right)}{\sqrt{1 + A - \sqrt{A^2 + A}}} \tag{20}$$

where

$$A = \zeta\frac{1 - \kappa}{\kappa} \tag{21}$$

Figure 6 shows the polyetic velocity of pandemic spread, V, as a function of the fraction of within-field spores, κ, for several values of the other parameters. As for the within-season velocity the polyetic velocity during successive seasons increases with increasing cropping ratio, ζ. Again, the polyetic velocity of pandemic spread increases with increasing effectiveness, $\sqrt{\alpha\Psi}$, of the disease. Both relations are biologically plausible.

Rate V increases with an increasing fraction of within-field spores, κ, except for values of κ close to unity. This remarkable relation was also found for the within-season rate, C, and the same explanation holds.

Decreasing the survival of foci, ε, over the off-season decreases the polyetic rate of pandemic spread. The push-back distance is independent of the parameter combination, $\alpha\Psi$, interpreted as a measure of effectiveness of the disease. Figure 6, however, shows that there is a large difference in the relative effect of ε for different values of the effectiveness. The survival of foci has a large influence on the polyetic velocity of pandemic spread, V, when the disease has a small $\sqrt{\alpha\Psi}T$ value. Measures to reduce

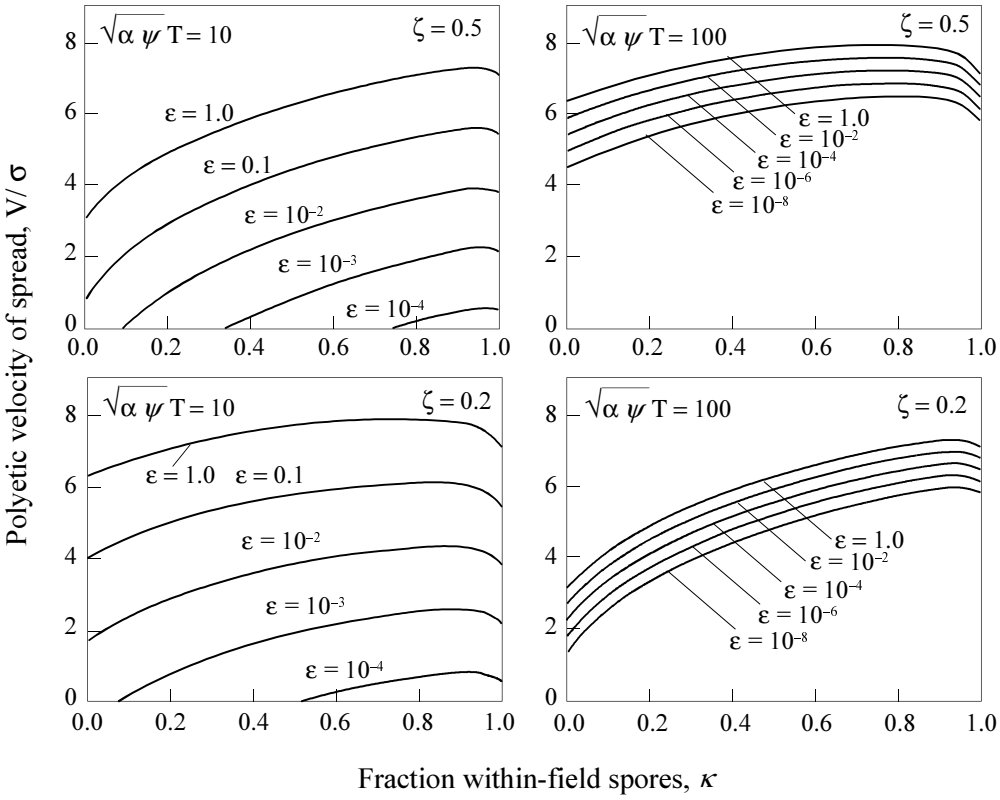

Figure 6. The polyetic velocity of pandemic spread (scaled by σ), V/σ, as a function of the fraction of within-field spores, κ. Parameters and function explained in Table 1.

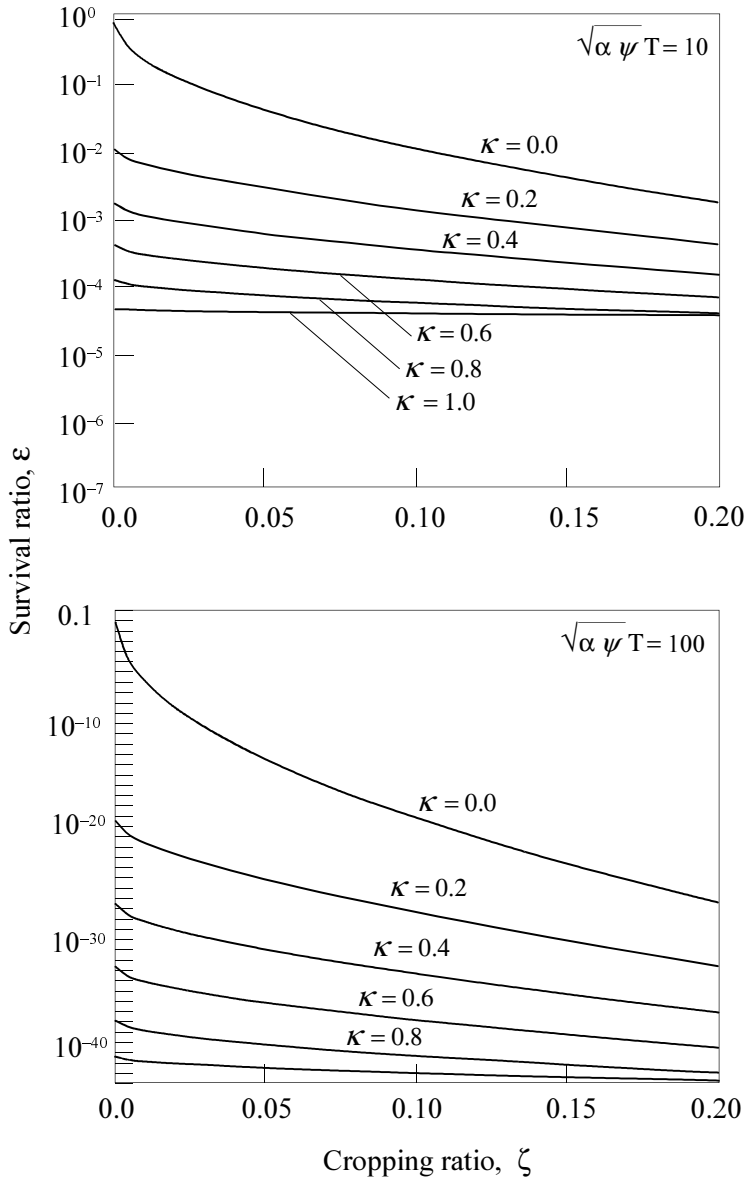

Figure 7. Boundary lines between expansion and extinction of the pandemic, x-axes – the fraction target area, ζ, y-axis – the threshold probability of survival ratio, ε. Above the boundary line the pandemic expands, below the line the pandemic is extinguished.

the velocity of disease spread by reducing survival during the crop-free period are thus successful only for diseases with small $\sqrt{\alpha\Psi}T$ values. The cropping ratio, ζ, does not seem to influence the reduction of the velocity V by sanitation during the crop-free period.

Decreasing survival of foci during the crop free period can reduce the rate of pandemic spread to zero, implying complete control of the disease. Setting V equal to zero in equation (20) we find the threshold value of the survival fraction, ε, where the rate of pandemic spread becomes zero. Complete control of the disease is attained when

$$\varepsilon \leq \exp\left\{-\sqrt{\alpha\Psi}\sqrt{\kappa}T\sqrt{1+A+\sqrt{A^2+A}}\right\} \tag{22}$$

Figure 7 shows the off-season survival ratio of foci, ε, as a function of the cropping ratio, ζ. The threshold value of ε depends to a minor extent on ζ. Only for κ values close to zero the necessary ε decreases considerably with increasing ζ. Figure 7 confirms that prevention of the pandemic by reducing ε only seems an interesting control strategy for pathogens with low effectiveness, i.e., diseases with low $\alpha\Psi$.

4 Discussion

This paper develops a framework for modeling the continental spread of focal plant disease. Methods to calculate the velocity of pandemic spread were developed both for within-season spread and for polyetic spread (during successive cropping seasons). To facilitate the study of the model by analytical methods, rather than by computer simulation, the information on the mechanisms underlying pandemic spread was stripped to bare essentials. Thus, several potentially important aspects are not yet incorporated in the present analysis.

Simplifications. In the model development we assumed the between-field-dispersal density to be rotationally symmetric. In real life, between-field spore dispersal will be far from rotationally symmetric due, e.g., to prevailing wind directions. The assumption of rotational symmetry can be relaxed easily and pandemic velocities calculated analytically. For details on these calculations consult Van den Bosch *et al.* (1990a) and Metz and Van den Bosch (1995). In development of the submodel for the between-field dispersal density, $D(\vec{x})$, preferential directions can be incorporated. In the example given to develop $D(\vec{x})$, such prevailing wind directions can be added by relaxing the assumption that after directional change the new direction is chosen randomly from all possible angles (Othmer *et al.*, 1988).

The model presented here is density independent. In reality, depletion of the disease-free space can occur. At the continental scale, density dependence will come into play at a certain position some time after the front of the pandemic has passed this position. Several related models for the spatial spread of populations show that the velocity of population spread is exactly the same in density dependent and density independent situations. Diekmann (1979) and Thieme (1977) proved this for density dependent variants of equation (5). Weinberger (1982) investigated a discrete time model of spatial spread and proved a similar theorem. For diffusion

models such behavior was demonstrated by Kolmogorov *et al.* (1937). These involved mathematical proofs have a biologically appealing result. A population spreads through space by intruding into areas where it was absent, the population wave being dragged forward by its tail. It is precisely the tail end that does not experience any density dependent effects since population densities are low.

Another simplification assumes that the cropping ratio, ζ, is constant throughout the continent. This is rarely true for agricultural crops. When tobacco blue mold, for example, invaded western Europe, tobacco production occurred in limited areas mainly whereas most of western Europe was mainly non-target area (Populer, 1964). Little is known about the effect of a heterogeneous environment on the spatial expansion of epidemics. Some analytical results were published by Shigesada *et al.* (1986, 1987). A further study of the spatial spread in heterogeneous environments is urgently needed.

Using only one parameter Ψ we assume that within-field and between-field spores have equal probability to initiate a new focus. This does however not imply that all between-field spores survive and are viable. The fraction of spores surviving dispersal can simply be seen as a correction factor to be incorporated in the function $g(a)$ describing spore production of a focus.

Dispersal models. As stated above, the calculation of the velocity of pandemic spread using equations (9) and (10) is possible only when the tails of the between-field dispersal density are exponentially bounded. Ferrandino (1993) developed a spore dispersal density with non-exponentially bounded tails based on detailed considerations of wind velocity and turbulence. This dispersal density was incorporated in an epidemic model. Numerical solutions of the model suggested that the velocity of epidemic spread increased continually. Ferrandino called such waves *dispersive epidemic waves.* In a recent paper, Kot *et al.* (1996) proved the existence of such dispersive waves in simple analytically tractable models of population invasions. They developed methods to approximate the velocity of the dispersive wave as a function of time since the introduction of the species.

Applications. The general model (4) can be adapted to describe a particular disease by an appropriate choice of $g(a)$ and $D(\vec{x})$. Detailed and realistic descriptions of the spore production function, $g(a)$, and the dispersal distribution, $D(\vec{x})$, will almost certainly be parameter rich. Parameter dependence of the velocity of pandemic spread is difficult to study in such parameter rich models. Therefore we restricted this first attempt at modeling pandemic spread to simple parameter sparse sub-models but in future research the introduction of more detailed models for $g(a)$ and $D(\vec{x})$ is useful. A guide to the development of models for between-field dispersal can be found in the work of Aylor (1986).

Simple analytically tractable models, as the one discussed in this paper, are useful tools to gain qualitative insight in the dependence of the velocity of pandemic spread on the underlying processes. Sometimes, such models can be put to work in real-life situations. The focus expansion model of van den Bosch *et al.* (1988a,b,c; 1990b) was validated using laboratory and field data. It will be difficult, if possible at all, to perform similar studies using the present model.

The authors think that the present model can best be used as a means to compare pandemics rather than as a stimulus to measure all input parameters experimentally.

Comparisons can be made, for example, between pandemics of a plant disease that invaded at various places in the world with different cropping ratios or different climatic conditions. Some general conclusions of a qualitative nature can be drawn. Containment of a quarantine disease will be more difficult when (1) its pandemic effectiveness is high, (2) the growing seaon is long, (3) the pandemic disease profile is shallow and (4) the off-season sanitation is poor.

Appendix I: Reformulating the Model

In this appendix we show that the model equations (4) are equivalent to the model equations (5) and (6). Taking Laplace transforms of the model equations (4) with respect to t we find

$$\begin{aligned} \overline{b}(s,\vec{x}) &= \Psi\overline{\nu}(s,\vec{x}) + \Psi\kappa\overline{b}(s,\vec{x})\overline{g}(s) \\ \overline{\nu}(s,\vec{x}) &= \zeta(1-\kappa)\int_{-\infty}^{\infty}\int_{-\infty}^{\infty}\overline{b}(s,\vec{x})\overline{g}(s)D(\vec{x},\vec{\varphi})d\varphi_1 d\varphi_2 \quad , \end{aligned} \tag{I.1}$$

where

$$\begin{aligned} \overline{b}(s,\vec{x}) &= \int_0^{\infty} e^{-st}b(t,\vec{x})dt \; ; \; \overline{\nu}(s,\vec{x}) = \int_0^{\infty} e^{-st}\nu(t,\vec{x})dt \; ; \; \overline{g}(s) \\ &= \int_0^{\infty} e^{-sa}g(a)da \quad . \end{aligned} \tag{I.2}$$

Solving for $b(s,\vec{x})$ in the first equation of (I.1) we find

$$\begin{aligned} \overline{b}(s,\vec{x}) &= \frac{\Psi\overline{\nu}(s,\vec{x})}{1-\Psi\kappa\overline{g}(s)} = \Psi\overline{\nu}(s,\vec{x})\sum_{i=1}^{\infty}\left(\Psi\kappa\overline{g}(s)\right)^{i-1} \\ &= \frac{\overline{\nu}(s,\vec{x})}{\kappa\overline{g}(s)}\sum_{i=1}^{\infty}\left(\Psi\kappa\overline{g}(s)\right)^{i} \quad . \end{aligned} \tag{I.3}$$

Substituting the second equation we find

$$\overline{b}(s,\vec{x}) = \zeta\Psi(1-\kappa)\int_{-\infty}^{\infty}\int_{-\infty}^{\infty}\frac{1}{\kappa}\overline{b}(s,\vec{x})\sum_{i=1}^{\infty}\left(\Psi\kappa\overline{g}(s)\right)^{i}D(\vec{x},\vec{\varphi})d\varphi_1 d\varphi_2 \quad , \tag{I.4}$$

and taking inverse Laplace transforms finally yields equations (5) and (6).

Appendix II: The Spore Dispersal Distribution

For a detailed account of the type of model formulation used in this appendix we refer the reader to the paper of Othmer, Dunbar and Alt (1988). We will use this method to derive the spore dispersal distribution.

A spore is dispersed by wind. It travels with velocity ν_1 in the x_1-direction and with velocity ν_2 in the x_2-direction. With a probability γ per unit of time the wind changes its direction. The new wind direction vector, (v_1, v_2), is chosen randomly from a distribution $Q(v_1, v_2)$. The spore is deposited on the surface with probability μ per time unit.

Denote by $p(t, x_1, x_2, v_1, v_2)$ the probability density of a spore to be at time t at position (x_1, x_2) and travelling with velocity vector (v_1, v_2). The spore dispersal process is governed by the model equation

$$\frac{\partial p(t, x_1, x_2, \nu_1, \nu_2)}{\partial t} = -\nu_1 \frac{\partial p}{\partial x_1} - \nu_2 \frac{\partial p}{\partial x_2} - \gamma p - \mu p + \gamma Q(\nu_1, \nu_2)$$

$$\int_{-\infty}^{\infty} \int_{-\infty}^{\infty} p(t, x_1, x_2, \nu_1', \nu_2') d\nu_1' d\nu_2' \tag{II.1}$$

Taking Laplace transforms with respect to time (s) and position (z_1, z_2) we find

$$s\overline{p}(s, \lambda_1, \lambda_2, \nu_1, \nu_2) - Q(\nu_1, \nu_2) = -\sum_i \nu_i \lambda_i \overline{p} - (\gamma + \mu)\overline{p} + Q(\nu_1, \nu_2)\gamma \overline{P} \tag{II.2}$$

with

$$P(t, x_1, x_2) = \int p(t, x_1, x_2, \nu_1', \nu_2') d\nu_1' d\nu_2' \tag{II.3}$$

The deposition kernel is then given by

$$\mu \overline{P} = \frac{\mu F(s, \lambda_1, \lambda_2)}{1 - \gamma F(s, \lambda_1, \lambda_2)} \tag{II.4}$$

where

$$F(s, \lambda_1, \lambda_2) = \int \int \frac{Q(\nu_1, \nu_2)}{\gamma + \mu + s + \sum \lambda_i v_i} dv_1 dv_2 \quad . \tag{II.5}$$

Assuming Q to be homogeneously distributed on the circle with radius ν we have

$$F(s, \lambda_1, \lambda_2) = \frac{1}{2\pi} \int_0^{2\pi} \frac{d\theta}{\gamma + \mu + s + \nu(\lambda_1 \cos(\theta) + \lambda_2 \sin(\theta))} \quad . \tag{II.6}$$

Now to calculate the Laplace transform of the marginal dispersal density put $\lambda_1 = \lambda$ and $\lambda_2 = 0$, substitute (II.6) into (II.4) to arrive at

$$\mu\overline{P} = \frac{1}{\sqrt{\left(\frac{\gamma+\mu+s}{\mu}\right)^2 - \left(\frac{\nu\lambda}{\mu}\right)^2} - \frac{\gamma}{\mu}} \quad . \tag{II.7}$$

The two special cases are found as follows:

1. Taking the limit for $\gamma \downarrow 0, \mu \to \infty$ and $\nu \to \infty$ such that ν/μ remains constant we find

   $$\mu\overline{P} = \frac{1}{\sqrt{1-\sigma^2\lambda^2}}$$

   where $\sigma^2 = \nu^2/\mu^2$, which is the Laplace transform of the marginal density of the rotationally symmetric exponential density (18).

2. Taking the limit for $\gamma \to \infty, \mu \to \infty$ and $\nu \to \infty$ such that $\nu^2/(\gamma\mu)$ remains constant we find

   $$\mu\overline{P} = \frac{1}{1-\frac{1}{2}\sigma^2\lambda^2}$$

   where $\sigma^2 = \nu^2/\gamma\mu$, which is the Laplace transform of the marginal density of the Bessel density (19).

References

Aylor, D. (1986) A framework for examining inter-regional aerial transport of fungal spores. *Agricultural and Forest Meteorology* **38**:263–288.

Cooke, M.C. (1891) Tobacco disease. *Gard. Chron.* **9**:173.

Diekmann, O. (1978) Thresholds and travelling waves for the geographical spread of infection. *Journal of Mathematical Biology* **6**:109–130.

Diekmann, O. (1979) Run for your life. *Journal of Differential Equations* **33**:58–73.

Fisher, R.A. (1937) The wave of advance of advantageous genes. *Annals of Eugenetics* **7**:355–369.

Ferrandino, F.J. (1993) Dispersive epidemic waves: I. Focus expansion within a linear plantation. *Phytopathology* **83**:795–802.

Gäumann, G.A. (1946) *Pflanzliche Infektionslehre*. Basel: Birkhauser. 611 pp.

Goldwasser, L., J. Cook and E.D. Silverman (1994) The effect of variability on metapopulation dynamics and rates of invasion. *Ecology* **75**:40–47.

Heesterbeek, J.A.P. and J.C. Zadoks (1987) Modelling pandemics of quarantine pests and diseases: problems and perspectives. *Crop Protection* **6**:211–221.

Kendall, D.G. (1965) Mathematical models of the spread of infection. In: *Mathematics and Computer Sciences in Biology and Medicine* (Medical Research Council, London, 213–224).

Kolmogorov, A., I. Petrovsky and N. Piscounov (1937) Etude de l'équation de la diffusion avec croissance de la quantité de matière et son application à un problème biologique. *Moscou University Bulletin of Mathematics* **1**:1–25.

Kot, M., M.A. Lewis and P. van den Driessche (1996) Dispersal data and the spread of invading organisms. *Ecology* **77**:2027–2042.

McGregor, R.C. (1978) People placed pathogens: The emigrant pests. In: *Plant Disease. An Advanced Treatise*, Vol. 2, p.383–396. (J.G. Horsfall and E.B. Cowling, eds) New York: Academic Press.

Metz, J.A.J. and F. van den Bosch (1995) Velocities of epidemic spread. In: *Epidemic Models: Their Structure and Relation to Data*. (D. Mollison, ed.) pp.150–186.

Minogue, K.P., Fry, W.E. (1983a) Models for the spread of disease: Model description. *Phytopathology* **73** 1168–1173.

Minogue, K.P., Fry, W.E. (1983b) Models for the spread of disease: Some experimental results. *Phytopathology* **73**:1173–1176.

Mollison, D. (1991) Dependence of epidemic and population velocities on basic parameters. *Mathematical Bioscience* **107**:255–287.

Othmer, H.G., S.R. Dunbar and W.Alt (1988) Models of dispersal in biological systems. *Journal of Mathematical Biology* **26**:263–298.

Populer, C. (1964) Le comportement des épidémies de mildiou du tabac, *Peronospora tabacina*. 1. La situation en Europe. *Bulletin de l'Institut agronomique et des Stations de recherches de Gembloux* **32**:339–378.

Press, W.H., B.P. Flannery, S.A. Teukolsky and W.T. Vetterling (1992) *Numerical Recipes in PASCAL: The Art of Scientific Computing*. Cambridge University Press. 759 pp.

Shigesada, N., K. Kawasaki and E. Teramoto (1986) Travelling periodic waves in heterogeneous environments. *Theoretical Population Biology* **30**:143–160.

Shigesada, N., K. Kawasaki and E. Teramoto (1987) The speed of travelling frontal waves in heterogeneous environments. In: *Mathematical Topics in Population Biology, Morphogenesis and Neurosciences*. (E. Teramoto and M. Yamaguti, eds) Lecture Notes in Biomathematics 71, Springer, Berlin, 88–97.

Skellam, J.G. (1951) Random dispersal in theoretical populations. *Biometrica* **38**:196–218.

Thieme, H.R. (1977) A model for the spread of an epidemic. *Journal of Mathematical Biology* **4**:337–351.

van den Bosch, F., J.C. Zadoks and J.A.J. Metz (1988a) Focus expansion in plant disease I: The constant rate of focus expansion. *Phytopathology* **78**:54–58.

van den Bosch, F., J.C. Zadoks and J.A.J. Metz (1988b) Focus expansion in plant disease II: Realistic parameter-sparse models. *Phytopathology* **78**:59–64.

van den Bosch, F., J.C. Zadoks and J.A.J. Metz (1988c) Focus expansion in plant disease III: Two experimental examples. *Phytopathology* **78**:919–925.

van den Bosch, F., J.A.J. Metz and O. Diekmann (1990a) The velocity of population expansion. *Journal of Mathematical Biology* **28**: 529–565.

van den Bosch, F., M. Verhaar, M.A. Buiel, A.A.M. Hoogkamer and J.C. Zadoks (1990b) Focus expansion in plant disease IV: Expansion rates in mixtures of resistant and susceptible cultivars. *Phytopathology* **80**:598–602.

Weinberger, H.F. (1982) Long-time behavior of a class of biological models. *SIAM Journal of Mathematical Analysis* **13**:353–396.

Zadoks, J.C. and P. Kampmeijer (1977) The role of crop populations and their deployment, illustrated by means of a simulator, EPIMUL76. *Annals of the New York Academy of Sciences* **287**:164–190.

Zadoks, J.C., Schein, R.D. (1979) *Epidemiology and Plant Disease Management*. Oxford University Press, New York. 427 pp.

Zadoks, J.C. and F. van den Bosch (1994) On the spread of plant disease: A theory on foci. *Annual Review of Phytopathology* **32**:503–521.